Process Safety and Environmental Protection 184 (2024) 271–283

Contents lists available at ScienceDirect

Process Safety and Environmental Protection

journal homepage: www.journals.elsevier.com/process-safety-and-environmental-protection

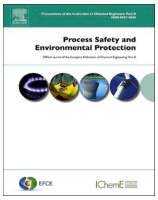

Sustainable emulsion treatment by volatilization enhanced by temperature and alkaline conditions in the remediation of a polluted landfill with lindane production wastes

J. Fernández[a], C. Herranz[b], A. Salvatierra[b], R. García-Cervilla[c], A. Santos[c], D. Lorenzo[c,*]

[a] *Dirección General de Calidad Ambiental, Gobierno de Aragón, Zaragoza, Spain*
[b] *Sociedad Aragonesa de Gestión Agroambiental, Gobierno de Aragón, Zaragoza, Spain*
[c] *Chemical Engineering and Materials Department, Facultad de Ciencias Químicas, Universidad Complutense de Madrid, Ciudad Universitaria S/N, 28040 Madrid, Spain*

ARTICLE INFO

Keywords:
Lindane wastes
Dehydrochlorination
Surfactant enhance aquifer remediation
Emulsion treatment
Volatilization

ABSTRACT

This study investigates the sustainable treatment of actual contaminated emulsions resulting from the injection of a non-ionic surfactant (Surfactant-Enhanced Aquifer Remediation, SEAR) in a landfill highly contaminated with residual dense non-aqueous phase liquid (DNAPL) from lindane wastes. Located in Bailin, Sabiñanigo, this landfill underwent SEAR treatment as part of the LIFE SURFING project in 2022. The DNAPL is a complex mixture, encompassing approximately 28 chlorinated organic compounds (COCs), including both aromatic (chlorobenzenes) and non-aromatic components (Hexachlorocyclohexanes, HCHs, and Heptachlorocyclohexanes, HeptaCHs). Notably, the non-aromatic compounds exhibit higher density and lower volatility than chlorobenzenes. SEAR-polluted emulsion can be treated by pollutant separation through volatilisation with an airstream. However, this method is limited to compounds with high-moderate volatility. Additionally, a decrease in vapour pressure is observed with increasing surfactant concentration. To overcome these limitations, simultaneous dehydrochlorination of HCHs and HeptaCHs, volatilisation of chlorobenzenes and emulsion breakage were carried out under alkaline conditions enhanced by temperature at a pilot scale using two real polluted emulsions from LIFE SURFING project. The intensified process demonstrated remarkable efficiency, eliminating over 90 % of COCs from the emulsion within 25 h of treatment. Furthermore, the pilot-scale results were used to validate a kinetic model developed here, predicting the hydrolysis rate of HCHs and HeptaCHs as a function of surfactant (1–10 g L^{-1}) and COCs (500–2500 mg L^{-1}) concentrations, temperature (25–60 °C), and alkali concentration (90–190 mM). This model and the previously established volatilisation kinetic model yield a good agreement between experimental and predicted data. The model constructed holds the potential to optimise treatment times and conditions for various pollutant and surfactant concentrations in emulsions during remediation.

1. Introduction

Persitent Organic Pollutants (POPs) are characterised by their persistence and toxicity in the environment since they are very resistant to chemical or biological degradation (Aidoo et al., 2023; Araújo et al., 2023; Duttagupta et al., 2020; Negrete-Bolagay et al., 2021). In addition, the POPs also present low solubility in water and form non-aqueous phase liquids (NAPLs).

An effective treatment to remediate polluted sites with NAPL is the application of surfactant enhancement aquifer remediation (SEAR) (Huo et al., 2020). This technique injects an aqueous solution containing a surfactant into the contaminated area. Then, a polluted stream is extracted with a mixture of organic compounds and the surfactant. Although SEAR is widely applied, the treatment presents a critical disadvantage. Using surfactants promotes the solubilisation and mobilisation of the NAPL to the aqueous phase, transferring the pollutants from a solid phase to the aqueous phase as an emulsion. Still, the contamination is not eliminated, and the emulsion must be correctly managed (Huo et al., 2020).

Several technologies have been applied to treat the emulsion obtained from SEAR. Selective oxidation of contaminants (Dominguez et al., 2019; García-Cervilla et al., 2021), selective membrane retention (Hanafiah et al., 2018; Trinh et al., 2019) or adsorption of organic

---

* Corresponding author.
E-mail address: dlorenzo@quim.ucm.es (D. Lorenzo).

https://doi.org/10.1016/j.psep.2024.01.083
Received 14 November 2023; Received in revised form 10 January 2024; Accepted 25 January 2024

Nomenclature

Abbreviations

AC	Activated Carbon
BDF	Cackward Differentiation Formulae
CI	Confidence Interval
COCs	Chlorinated Organic Compounds
CMC	Criticar micellar concentration
DCB	Dichlorobenzene
DNAPL	Dense Non Aqueous Phase Liquid
E3	E-Mulse® 3
ECD	Electron Capture Detector
FID	Flame Ionisation Detector
GC	Gas Chromatography
GDP	Global Disjunctive Programming
HCH	Hexachlorobenzene
HeptaCH	Heptachlorobenzene
HexaCX	Hexachlorocyclohexene
ISTD	Internal standard
MSD	Mass spectrometer detector
NAPL	Non Aqueous Phase Liquid
PentaCX	Pentachlorocyclohexene
POP	Persistent Organic Pollutant
SEAR	Surfactant Enhanced Aquifer Remediation
ST	Surface Tension
TCB	Trichlorobenzene
TetraCB	Tetrachlorobenzene

Symbols

a	Fitting parameter
b	Fitting parameter
C	Concentration in $mmol\cdot L^{-1}$ for COCs in aqueous phase, $mmol\cdot kg^{-1}$ in DNAPL, $g\cdot L^{-1}$ for surfactant and NaOH in aqueous phase and $mg\cdot L^{-1}$ for total DNAPL in solution
c	Fitting parameter
CMC	Critical Micelle Concentration ($mg\cdot L^{-1}$)
d	Fitting parameter
e	Fitting parameter
E_a	Activation energy (K)
ESC	Equivalent Surfactant Concentration ($mg\cdot L^{-1}$)
f	Fitting parameter
F_{gas}	Gas molar flow ($mol\cdot h^{-1}$)
H_{app}	Apparent Henry's law constant (atm)
k	Kinetic constant
k_0	Pre-exponential factor for k
MSR	Molar Solubilization Ratio ($mol\cdot g^{-1}$)
n	molar quantity ($mmol$)
P	Pressure (atm)
Q_{air}	Flow rate of air ($L\cdot h^{-1}$)
R	Production rate ($mmol\cdot L^{-1}\cdot h^{-1}$)
r	Reaction rate ($mmol\cdot L^{-1}\cdot \mathrm{min}^{-1}$)
SQR	Sum of quadratic residuals
t	time (h)
T	Temperature (K)
T_v	Temperature on volatization (℃)
V	Vaporisation rate ($mmol\cdot L^{-1}\cdot h^{-1}$)
$V_{emulsion\ in\ chamber\ 1}$	Volume of emulsión in chamber 1 (L)
V_L	Total volume (L)
X	Conversion
x	Molar fraction in liquid phase
xr	Residual surfactant with temperature
y	Molar fraction in gas phase
Y	Production fraction ($mmol\cdot L^{-1}$)

Greek letters

α	Fitting parameter
β	Fitting parameter
υ	Stoichiometric coefficient
Γ	Disjuntive binary parameter

Subscripts

1	Reaction of dehydrochlorination of HCHs
2	Reaction of dehydrochlorination of PentaCXs
3	Reaction of dehydrochlorination of HeptaCHs and HexaCXs
α-HCH	Isomer alpha of HCH
DCBs	Sum of all isomers of DCB
δ-HCH	Isomer delta of HCH
DNAPL	Sum of all COCs present in DNAPL
ε-HCH	Isomer epsilon of HCH
ESC	Equivalent Surfactant Concentration
exp	Experimental value
γ-HCH	Isomer gamma of HCH (Lindane)
HCH	Sum of all isomers of HCH
HeptaCH	Sum of all isomers of HeptaCH
i	Reaction number
j	Any COC
k	Each isomer of the any j compound
NaOH	Sodium hydroxide
o	Initial
PentaCXs	Sum of all isomers of PentaCXs
precipitated	Compound not in solution
pred	Predicted value
R	Total number of reactions
S	Surfactant
sol	Compound in solution
T	Total
t	Discrete time value
TCBs	Sum of all isomers of TCB
teo	Teorical value
TetraCBs	Sum of all isomers of TetraCB

pollutants on activated carbon (Rosas et al., 2013) have been effectively applied. In the latter process, the polluted emulsion is directly sent to adsorption on activated carbon (AC), and the efficiency of the process remarkably decreases due to the quick saturation of AC with the surfactant (Rosas et al., 2013). The efficiency and economy of further pollutant adsorption on activated carbon can be improved by treating the emulsion with air stripping to transfer the volatile compounds from the aqueous solution to an air stream, and it could be effective when the organic compounds are volatile or semivolatile (Huan and Shang, 2006).

Recent studies have explored the selective volatilization of chlorinated organic compounds (COCs) from emulsions containing an aqueous surfactant solution and a mixture of chlorobenzene and dichlorobenzene isomers (DCBs) (Sáez et al., 2022b). Similarly, a complex emulsion comprising trichlorobenzenes (TCBs), tetrachlorobenzenes (TetraCBs), hexachlorocyclohexanes (HCHs), pentachlorocyclohexenes (PentaCXs), heptachlorocyclohexanes (HeptaCHs), hexachlorocyclohexanes (HexaCXs) isomers, and the surfactant E-Mulse® 3 (E3) under alkaline conditions has been investigated (Sáez et al., 2022a). In the latter work, the emulsion previously alkalinised, promoting the dehydrochlorination of HCHs and PentaCXs to TCBs and

HeptaCHs and HexaCXs to TetraCBs whose boiling points are lower than the parent COCs.

The effectiveness of using alkaline conditions dealing with HCHs has also been confirmed by Bouzid et al. (2021), who focused on the alkaline degradation of HCHs in contaminated sandy soils. In a xanthan solution, they injected a $Ca(OH)_2$ suspension into the ground. The findings of the study revealed that the degradation kinetics of HCH followed a pseudo-first-order reaction, meaning that the degradation rate depended on their concentration and followed a first-order rate equation. However, the dehydrochlorination kinetic of HCHs and HeptaCHs in the micelles as a function of variables that can affect the rate has not been addressed.

The primary objective of this study is to assess the efficacy of treating real SEAR emulsions obtained from the LIFE SURFING project (2020–2022). This Project, carried out at the Bailin Landfill in Sabiánigo, Spain, was a notable endeavour to rehabilitate a contaminated fractured aquifer polluted by a dense NAPL (DNAPL) contamination from a neighbouring lindane manufacturing site. To overcome the limits of existing extraction methods, the Project used new techniques, SEAR and in situ chemical oxidation enhanced by surfactant (S-ISCO). Two SEAR tests were done in the spring of 2022 using E-3, which successfully recovered about 130 kg of DNAPL.

Furthermore, the experimental data obtained from the pilot plant studies were used to verify the effectiveness of a proposed model that incorporates the dehydrochlorination kinetic model for non-aromatic compounds (HCHs, PentaCXs, HeptaCHs, and HexaCXs) and the vaporization of aromatic compounds (TCBs, TetraCBs, and DCBs) (Sáez et al., 2022a). This work presents a kinetic model that can account for the transformation of HCHs and PentaCXs into TCBs and HeptaCHs and HexaCXs into TetraCBs, based on experimental data collected under various conditions of temperature, surfactants, sodium hydroxide NaOH, and initial concentrations COCs. The vaporization and alkalinization model was designed to predict the evolution of emulsions under a wide range of variable conditions, allowing for the optimization of treatment conditions for each case.

2. Materials and methods

2.1. Chemicals

The quantification of COCs was performed using calibration curves prepared from commercial compounds (Sigma Aldrich, analytical grade): chlorobenzene (CB), 1,2-dichlorobenzene (1,2-DCB), 1,3-dichlorobenzene (1,3-DCB), 1,4-dichlorobenzene (1,4-DCB), 1,2,3-trichlorobenzene (1,2,3-TCB) 1,2,3,4-tetrachlorobenzene (1,2,3,4-TetraCB), 1,2,3,5-tetrachlorobenzene (1,2,3,5-TetraCB), and 1,2,3,4- tetrachlorobenzene (1,2,3,4-TetraCB), hexachlorocyclohexane isomers (α, β, γ, δ and ε-HCH). Additionally, the limonene ((R)-(+)-Limonene, Sigma Aldrich) (cosolvent of surfactant) was also calibrated. Bicyclohexyl ($C_{12}H_{22}$, Sigma Aldrich) and tetrachloroethane ($C_2H_2Cl_4$, Sigma Aldrich) were used as internal standards (ISTD) for quantification by gas chromatography (GC).

The pilot plant experiments utilised two distinct real streams derived from the SEAR treatment within the LIFE SURFING project (https://lifesurfing.eu/), with their characterisation detailed in Table S1 (runs PP1 and PP2). This table includes information on surfactant and organic phase concentrations and a summary of the molar fraction of the emulsion COCs.

The surfactant selected was E-Mulse® 3 (EthicalChem), which is a non-ionic surfactant with a critical micelle concentration (CMC) of $80 mg \cdot L^{-1}$. E3 was selected because it is a biodegradable and non-toxic surfactant (Santos et al., 2019) and has been successfully applied in the solubilisation of COCs from this DNAPL to the aqueous phase (García-Cervilla et al., 2020).

The DNAPL extracted from the subsoil of the Bailin Landfill in Sabiñánigo, Spain, as part of the LIFE SURFING project, served as the basis for kinetic experiments involving the dehydrochlorination of HCHs and HeptaCHs in the presence of surfactant. The composition of DNAPL is detailed in Table S2 of the Supplementary Material. NaOH was employed to facilitate alkaline dehydrochlorination.

Sulfuric acid (Sigma Aldrich, 96 %) was used to stop the dehydrochlorination reaction, and the reaction samples were diluted in methanol (Sigma Aldrich, HPLC grade) before their analysis.

2.2. Experimental procedures

The experimental procedure was divided into two sets. The first one (Set-A) studied the treatment of the actual streams obtained after applying SEAR in the Bailin Landfill at the pilot plant scale. The second set (Set-B) investigated the effect of the temperature, NaOH and surfactant concentrations in the dehydrochlorination rate of HCHs and PentaCXs to TCBs and HeptaCHs, and HexaCXs to TetraCBs.

2.2.1. COCs dehydrochlorination and volatilisation at pilot plant experiments (Set-A)

The remediation of the Bailin landfill (Sabiñanigo, Spain) highly contaminated with DNAPL from lindane liquid wastes, was carried out as part of the LIFE SURFING project. Surfactant-enhanced aquifer Remediation (SEAR) technology was employed as an initial step to effectively remove a significant portion of the residual DNAPL present in the sandstone fractures beneath the landfill. This procedure entailed injecting a surfactant aqueous solution and extracting a contaminated fluid containing the liquid organic phase (as mobilised DNAPL) and an aqueous polluted emulsion with surfactant and dissolved COCs (COCs solubilisation). The polluted emulsion underwent a treatment process involving alkalinisation and air stripping enhanced by temperature to facilitate the volatilisation of COCs within the aqueous emulsion and the emulsion breakage. The resulting polluted gas stream containing volatilised COCs was subsequently guided through an AC filter, ensuring effective capture and retention of these compounds.

The treatment of two emulsions obtained during the SEAR process (PP1 and PP2, with composition in Table S3) was carried out in a double-chamber reactor (volume), the first with aeration and the second without aeration, avoiding the foam exit with the gas phase. Alkali (NaOH, 25 % aqueous solution) was initially added and supplied to the chamber when necessary using a pulse pump to maintain the pH above 12. The aqueous phase was recirculated from the second chamber to the first one, with external heating (two 24 kW heaters). Antifoam was introduced into the recirculated fluid via a dosing pump to avoid foam formation. The aqueous phase is recirculated to the reactor, passing through a diffuser nozzle. The tiny droplets formed promote foam disruption and volatilisation of lighter organics. The volatilised COCs exited the second chamber with the air stream, captured in two consecutive activated carbon filters. The tank temperature was maintained at 50°C throughout the process. Emulsion samples were collected and analysed during 0 to 100 h to quantify COCs using the previously outlined procedure. Experimental conditions of runs PP-1 and PP-2 are summarised in Table S3. A schematic representation of this process is presented in Fig. 1.

2.2.2. COCs alkaline hydrolysis (Set-B)

The dehydrochlorination of HCHs and PentaCXs to TCBs and HeptaCHs, and HexaCXs and HeptaCHs to TetraCBs were conducted in batch mode using sealed 20 mL Teflon vials without headspace closed with Teflon caps magnetically stirred. 11 runs were carried out. A certain amount of DNAPL-1 (500–1000 mg/L) and surfactant E-Mulse® 3 (1 to 10 g/L) were added to 19 mL of milli-Q water. Then, the vials were heated in a thermostatic bath to obtain the desired temperatures (25 °C - 60 °C). Once the temperature was reached, 1 mL of NaOH solution was added (zero time) into the vials with the final NaOH concentration in the 90–190 mM range. The experimental conditions of the runs are

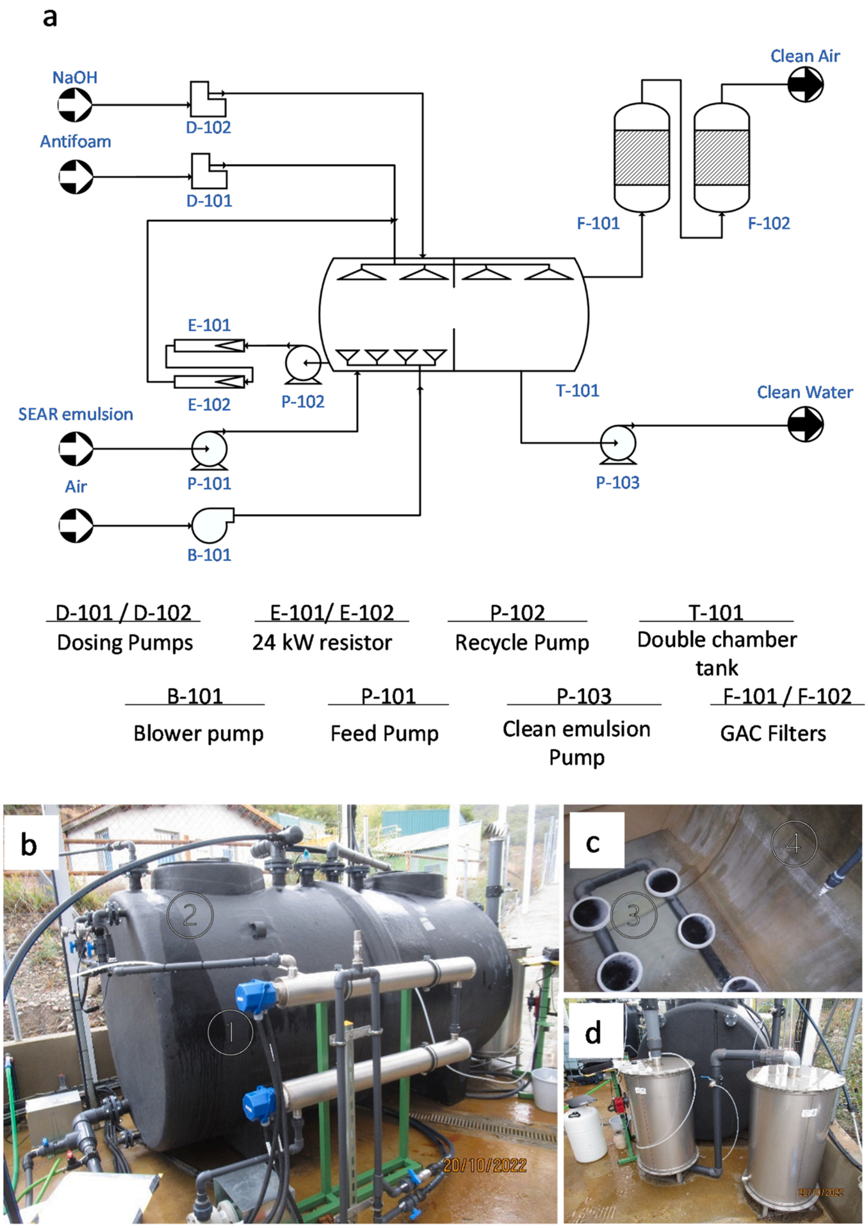

Fig. 1. a) Schematic representation of pilot plant where the experiments in Set-A were carried out, b) double chamber vaporisation unit, c) inside of the first chamber vaporisation unit and d) activated carbon filters. 1: E-101, E-102 24 kW resistors; 2: Doble chamber evaporation unit; 3: air diffusers 4: spray system for emulsion feed.

summarised in Table S4. A vial was sacrificed at each reaction time, and the content was immediately analysed. For this analysis, 1 mL of the emulsion was neutralised with 1 mL of H_2SO_4 0.1 M, then diluted 1:10 v:v in methanol and analysed by gas chromatography coupled with flame ionization and electron capture detectors (GC-FID/ECD). Each reaction was carried out in triplicate, finding deviations lower than 10 %. The surfactant concentration in each reaction sample was determined by measuring the equivalent surfactant concentration (ESC) with 5 mL of the emulsion each time. ESC accounted for the concentration of E3 and any byproducts generated from the reaction with NaOH that retained surfactant capacity. ESC was calculated by measuring the critical micelle concentration (CMC) of the reaction sample using a Krüss tensiometer (Hamburg, Germany). The CMC was determined as the intersection between the regression line of the region where concentration and surface tension (ST) are linearly dependent and the straight line passing through the plateau where ST is independent of concentration. The ratio of the CMC of the reaction sample to the CMC of pure E3 represented the dilution factor of the initial surfactant concentration. The product of this dilution factor and the initial surfactant concentration yielded the ESC (Dominguez et al., 2019).

2.3. Analysis

The concentration of COCs in the emulsion in Set-A and Set-B experiments was analysed by gas chromatography. Aqueous samples (after neutralisation) were diluted 1:10 in methanol and immediately injected in a GC-FID/ECD (Agilent 8860) with an autosampler (Agilent GC Sampler 120). The column was Agilent HP5-MSUI (19091S-433UI, 30 m x 0.25 mm ID x 0.25 μm). Helium was used as carrier gas with a flow rate of 2.9 $mL\cdot\text{min}^{-1}$. 2 μL of each reaction sample were injected in the GC injection port at 250 ℃. The GC oven worked at a programmed temperature gradient, starting at 80 ℃ and raising the temperature at a rate of 15℃$\cdot\text{min}^{-1}$ until 180 ℃, and then keep it constant for 15 min. Additionally, a split ratio of 10:1 was employed in the analysis (Santos et al., 2018). A GC coupled with a mass spectrometer detector (MSD) was used to identify reaction intermedia using the same method. The pH was analysed in all experiments with a Metrohm 914 pH/conductometer.

3. Results and discussion

3.1. Pilot plant experiments

The real SEAR emulsions obtained from the LIFE SURFING project were treated in the pilot plant schematised in Fig. 1, and the experiments are summarised in Table S3. The composition of COCs in emulsion is summarised in Table S1, as is shown the initial emulsion is composed of DCBs, TCB and TetraCB isomers as aromatic compounds and HCHs, PentaCXs, HeptaCHs, and HexaCXs as non-aromatic compounds.

In these experiments, the remaining concentrations of surfactant and COCs, calculated with Eq. (1) were monitored over time. Fig. 2 illustrates the concentration of DNAPL, calculated as the sum of COCs and surfactant concentrations.

$$\left(1 - X_j\right) = \frac{\sum C_k}{\sum C_{ko}} \tag{1}$$

where $1 - X_j$ is the remaining fraction of the compound j in the emulsion, and C_k and C_{ko} are the concentration in $mmol{\cdot}L^{-1}$ of the isomers at the specific and initial times, respectively. If $\mathrm{j} = \mathrm{HCH}$, then $\mathrm{k} = \alpha - HCH$, $\gamma - HCH$, $\delta - HCH$, $\varepsilon - HCH$; if $\mathrm{j} = \mathrm{HeptaCH}$ then $\mathrm{k} = HeptaCH - 1, HeptaCH - 2, HeptaCH - 3 and\ a - HexaCX, b - HexaCX, c - HexaCX, d - HexaCX, e - HexaCX$ If $\mathrm{j} = \mathrm{PentaCX}$ then $\mathrm{k} = \gamma - PentaCX, \delta - PentaCX, \beta - PentaCX, \eta - PentaCX, \theta - PentaCX$; $\mathrm{j} = \mathrm{TetraCBs}$ then $\mathrm{k} = TetraCB - a, TetraCB$; $\mathrm{j} = 1,3,5 - TCB, 1,2,4 - TCB, 1,2,3 - TCB$ and $\mathrm{j} = \mathrm{DCB}$ $\mathrm{k} = 1,3 - DCB, 1,4 - DCB, 1,2 - DCB$.

As shown in Fig. 2, after 40 h of treatment, the remaining fraction of COCs in the emulsion was lower than 0.05 for experiments PP-1 and PP-2 (95 % of total DNAPL reduction). The experimental conditions used in PP-1 and PP-2 were similar. The main difference was the surfactant concentration. According to the experimental results, the increase in the surfactant concentration (PP-2) results in lower volatilisation of DNAPL with a negligible effect on the surfactant conversion.

The remaining concentration profiles of HCHs, PentaCX and HeptaCH (as the sum of HeptaCH and HexaCXs isomers) are plotted in Fig. 3. As shown, these chemicals were wholly eliminated in the early stages of treatment. The latter can be explained by the fact that these isomers make up the non-aromatic component of the DNAPL and have higher boiling points than aromatic compounds. Therefore, their elimination can be attributed to the dehydrochlorination reaction.

The hydrolysis of non-aromatic compounds was unaffected by the surfactant concentration (0.58 g/L in PP-1 and 1.49 g/L in PP-2). The remaining concentration profiles of the most volatile compounds, TCBs, TetraCBs, and DCBs, are plotted in Fig. 4. The remaining concentration profiles of TCBs and TetraCBs isomers (symbols in Fig. 4a and Fig. 4b) showed a maximum greater than 1. This fact supports the idea that such chemicals are generated through the dehydrochlorination of non-aromatic compounds and removed through air stripping., in agreement with the experimental results observed in the vaporization of non-aromatic compounds (Sáez et al., 2022a). Early in the process, the maximum was present, indicating that hydrolysis happened faster than vaporisation.

3.2. Model of SEAR emulsion post-treatment by vaporisation

The design of the volatilisation step to treat the emulsion from the SEAR tests of the LIFE SURFING requires the modelisation of an intensified operation where the hydrolysis of non-aromatic compounds and the vaporisation of aromatic compounds occur, taking into account the stability of the surfactant using airflow. The inputs of the model will be the operation conditions of the unit, such as temperature, airflow and the treated volume and the chemical characterisation of the emulsion, comprising the surfactant and DNAPL concentrations and the mass / molar fractions of the different COCs in the DNAPL.

The model proposed considered the following assumptions:

- An apparent Henry's law constant describes the vapour-liquid partitioning of chlorinated solvents in surfactant solutions (Vane and Giroux, 2000). The apparent Henry's law constants were calculated using Eq. (2). This equation takes into account the effect of temperature (T_V in °C) and surfactant concentration (CS in $g{\cdot}L^{-1}$)on the vaporization of CB, 1,2-DCB, 1,4-DCB, 1,2,4-TCB, 1,2,3-TCB, a-TetraCB and b-TetraCB. The parameters of Eq. (2) were estimated in previous works (Sáez et al., 2022a; Sáez et al., 2022b) summarised in Table S5.

$$H_{app,j} = \exp\left(a + b{\cdot}C_S + c{\cdot}T_V + d{\cdot}{C_S}^2 + e{\cdot}T_V^2 + f{\cdot}C_S{\cdot}T_V\right) \quad atm$$

$$j = \{\mathrm{CB}, 1,2 - \mathrm{DCB}, 1,4 - \mathrm{DCB}, 1,2,4 - \mathrm{TCB}, 1,2,3 - \mathrm{TCB}, \mathrm{a} - \mathrm{TetraCB}, \mathrm{b} - \mathrm{TetraCB}\} \tag{2}$$

- HCHs, HeptaCH, HexaCX and PentaCX, were not vaporised under the experimental operation conditions. The apparent Henry's law constant is almost zero, as is expressed in Eq. (3).

$$H_{app,j} = 0 j \in \{HCH, HeptaCH, HexaCX, PentaCX\} \tag{3}$$

- The CB, DCBs, TCBs, and TetraCBs isomers do not suffer the dehydrochlorination reaction. The kinetic constant of those compounds is zero, as expressed in (4).

$$k_k = 0 \quad k \in \{\mathrm{DCB}, \mathrm{CB}, \mathrm{TCB}, \mathrm{TetraCB}\} \tag{4}$$

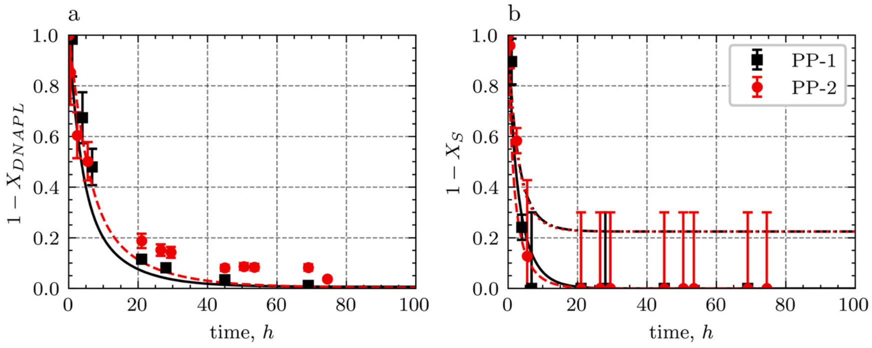

Fig. 2. The remaining concentration profiles of a) DNAPL as the sum of COCs and b) surfactant in pilot plant experiments are summarised in Table S4. Symbols depict experimental values and line the predicted values using the vaporisation and dehydrochlorination intensified model.

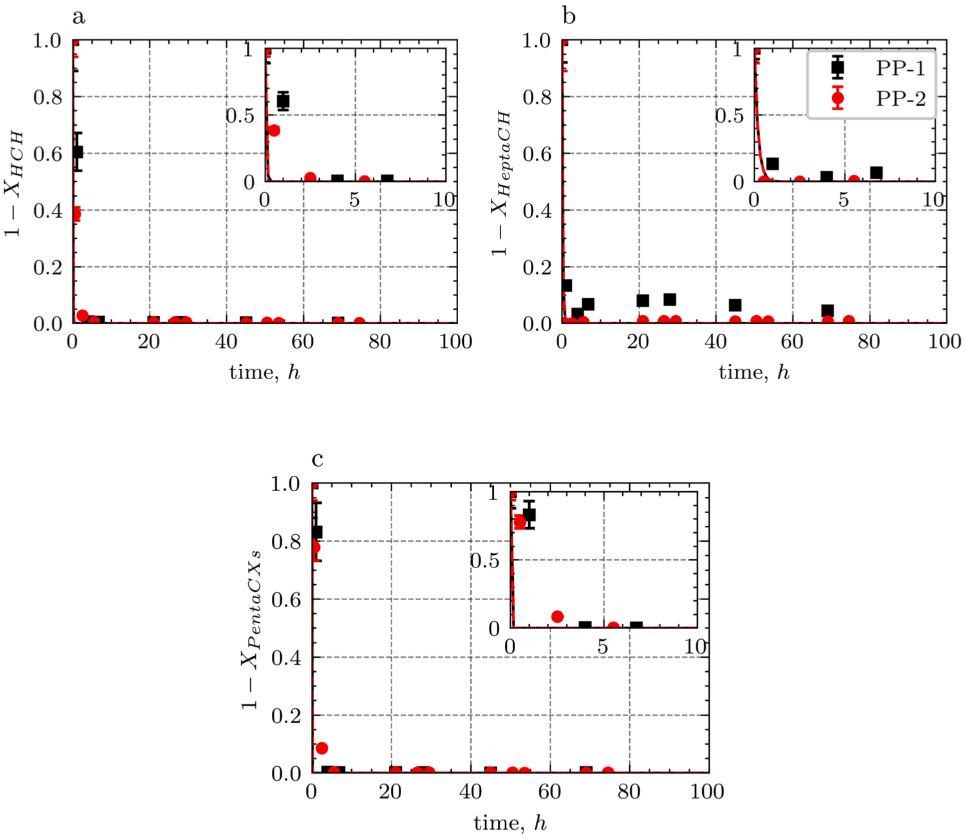

Fig. 3. The remaining concentration profiles of a) HCHs; b) HeptaCH + HexaCX and c) PentaCX as the sum of isomers in pilot plant experiments, are summarised in Table S4. Symbols depict experimental values and line the predicted values using the vaporisation and dehydrochlorination intensified model.

- The reaction rate for the dehydrochlorination of HCHs, PentaCX isomers, and the sum of HeptaCH and HexaCX must be greater than 0. The reaction rate must be measured experimentally in the surfactant presence.

$$k_k > 0 \quad k \in \{\text{HCHs, PentaCX, HeptaCH and HexaCX}\} \tag{5}$$

- The reaction of E3 and NaOH promoted the loss of the surfactant capacity, affecting the maximum DNAPL that can be solubilised and then its precipitation (Sáez et al., 2022a).

The vaporisation and dehydrochlorination mass balance can be modelled using Eq. (6).

$$\frac{dC_j}{dt} = R_j + V_j \tag{6}$$

being R_j and $V_j$the production and the vaporisation rates of compound j in $mmol{\cdot}L^{-1}{\cdot}h^{-1}$, respectively. The molar balance for the COC volatilised with time can be determined using Eq.(7).

$$-\frac{dn_j}{dt} = -\frac{V_L C_T dx_j}{dt} \tag{7}$$

being n_j of the amount of mol of compound j; V_L is the total volume of emulsion treated in L; C_T is the total concentration of the emulsión, mainly composed of water, and it can be considered constant and equal to 55000 $mmol{\cdot}L^{-1}$; Finally x_j is the molar fraction of compound j in the liquid phase.

Assuming that the gas flow leaving the operation unit is in equilibrium with the emulsion by applying the Raoult law, the molar fraction of compound j in the gas phase is computed using Eq. (8).

$$y_j = \frac{H_{app,j}{\cdot}x_j}{P_T} \tag{8}$$

being P_T the total pressure in atm. Eq. (7) and Eq. (8) can be used to express the equilibrium condition between the gas and liquid phase in the operation unit:

$$-\frac{V_L{\cdot}C_T{\cdot}dx_j}{dt} = F_{gas}{\cdot}y_j = \frac{F_{gas}H_{app,j}x_j}{P_T} \tag{9}$$

here, F_{gas}represents the gas molar flow rate in $mmol{\cdot}h^{-1}$. Supposing the total concentration of the liquid phase, mainly water, was constant, Eq. (10) can be expressed as the volatile compounds' vaporisation rate.

$$V_j = \frac{dC_j}{dt} = -\frac{F_{gas}H_{app,j}C_j}{V_L{\cdot}C_T{\cdot}P_T} \tag{10}$$

The reaction rate of the different compounds can be expressed as follows:

$$R_{ij} = \sum_{i=1}^{R} \upsilon_{ij} k_{ij} C_{NaOH}^{m} C_j \tag{11}$$

As was set in a previous work, surfactant capacity was affected by temperature and surfactant concentration. The mass balance of the ESC can be calculated using the kinetic model expressed in Eq. (12), whose parameters and equations were obtained by Sáez et al. (2022a) and those are summarised in Table S6.

$$-\frac{dC_{ESC}}{dt} = k(C_{ESC} - C_{So}x_r)\frac{(1 + k_1 C_{DNAPL})}{(1 + k_2 C_{DNAPL})} \quad t = 0 \therefore C_{ESC} = C_{So} \tag{12}$$

In Eq. (12) x_r represents the residual ESC with temperature, as shown in Table S6. As depicted in Fig. 2, the experimentally obtained ESC was

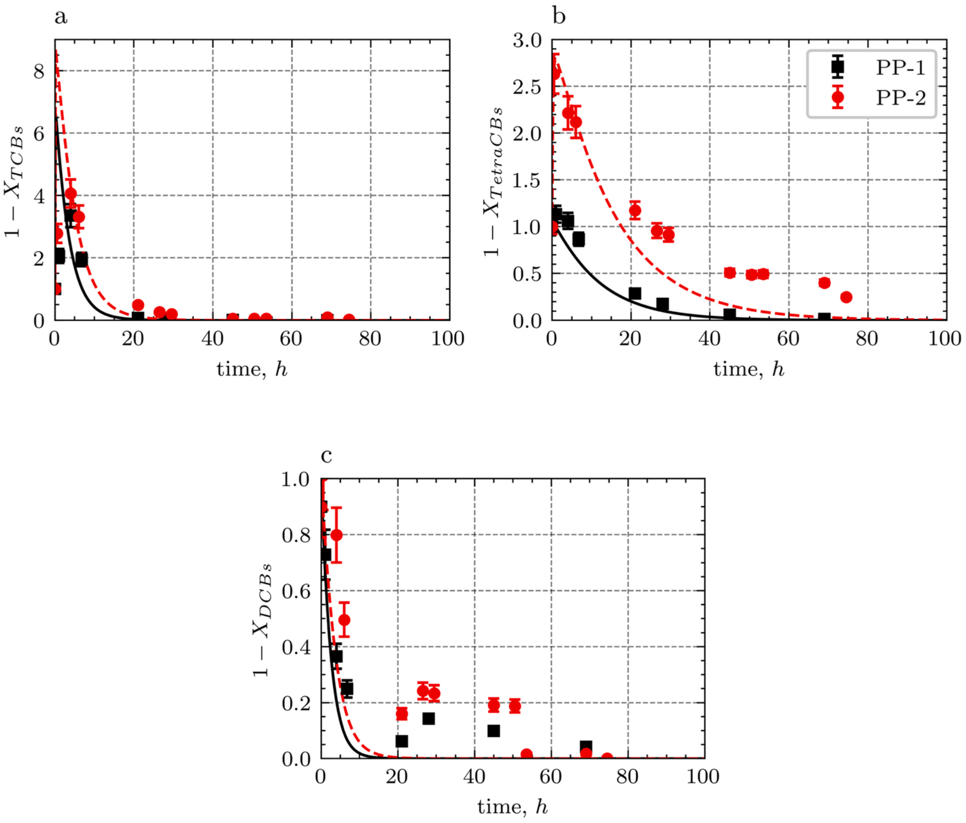

Fig. 4. The remaining concentration profiles of a) TCBs, b) TetraCBs and c) DCBs as the sum of isomers in pilot plant experiments are summarised in Table S4. Symbols depict experimental values and line the predicted values using the vaporisation and dehydrochlorination intensified model.

negligible for PP-1 and PP-2. This could be due to errors in the determination method (concentration below the detection limit) or insignificant residual ESC under the tested conditions. Therefore, it was calculated using both scenarios: using x_r as a function of temperature and $x_r = 0$ in Eq. (12).

3.3. Kinetic of dehydrochlorination of non-aromatic COCs

The kinetics of dehydrochlorination for non-aromatic chlorinated organic compounds (PentaCXs and HCHs to TCBs and HexaCXs and HeptaCHs to TetraCBs) were investigated at several temperatures, surfactant and COCs concentrations, and alkali concentrations, as summarised in Table S4.

3.3.1. Product distribution

The reaction samples were analyzed by GC/MDS to identify subproducts of the dehydrogenation reaction. No compounds other than those that compound the DNAPL samples (detailed in Table S2) were identified.

The quantification of the reaction samples showed that the concentration of the non-aromatic compounds (HCH, HeptaCH, HexaCX and PentaCX) decreased with time. In contrast, the TCB and TetraCBs isomer concentration increased with reaction time. Furthermore, the concentration of DCB isomers was not modified.

The results indicated that the number of reacted HCH and PentaCX molecules equated to the number of moles of TCBs generated (as the sum of isomers). Moreover, the variation in the moles of HeptaCH and HexaCX caused the same quantity of TetraCBs. The same conclusion was confirmed by Bouzid et al. (2021) and documented elsewhere (García-Cervilla et al., 2021; Lorenzo et al., 2020), where various soil samples contaminated with a DNAPL from Sabiñanigo landfills (similar composition to those detailed in Table S2), were exposed to an alkaline solution (pH > 12) for 48 h.

The dehydrochlorination mechanism of HCH and HeptaCH with NaOH was explained as a nonreductive elimination, also known as β-elimination (Bescós et al., 2021; Bouzid et al., 2021; Li et al., 2011; Verma et al., 2023; Zhang et al., 2023). This mechanism involves the loss of a halogen and a neighbouring proton to form an alkene, following the E2 mechanism. For the HCHs, β-elimination is expected to be a facile process due to the relative acidity of the hydrogen on the adjacent, or beta carbon to that bearing the departing halogen (Ingold, 1953; Li et al., 2011).

The first dehydrohalogenation step of HCH produces PentaCX isomers. Successive β-eliminations would progress through a relatively unstable tetrachlorocyclohexadienes (TetraDiCX, this compound was not experimentally identified in runs in Tabls S4) to TCBs isomers, which would be expected to be relatively stable by the aromatic nucleus. (Bescós et al., 2021; Li et al., 2011).

Scheme 1 shows the dehydrochlorination reaction, where a series of reactions was presented, starting with HCH and finishing in TCBs isomers. The same model was proposed by HeptaCH, as summarised in Scheme 2.

3.3.2. NaOH concentration effect

The effect of NaOH concentration in the dehydrochlorination reaction was investigated using 90 and 190 mM of NaOH (3.6 and 7.6 $g{\cdot}L^{-1}$ of NaOH, respectively and pH>12) and surfactant and DNAPL concentrations of 5 $g{\cdot}L^{-1}$ and 500 $mg{\cdot}L^{-1}$ at 25 °C. In Fig. 5a, the remaining profiles of HCH, as the sum of isomers to TCBs, are depicted as symbols. In addition, Fig. 5b illustrates the remaining fraction of the sum of HeptaCH isomers to TetraCBs, and Fig. 5c shows the evolution of PentaCXs. The remaining fraction profiles $(1 - X_j)$ of those compounds were calculated using Eq.(1). HeptaCH and HexaCX are lumped since the concentration of HexaCX isomers was lower than 20 % of HeptaCHs.

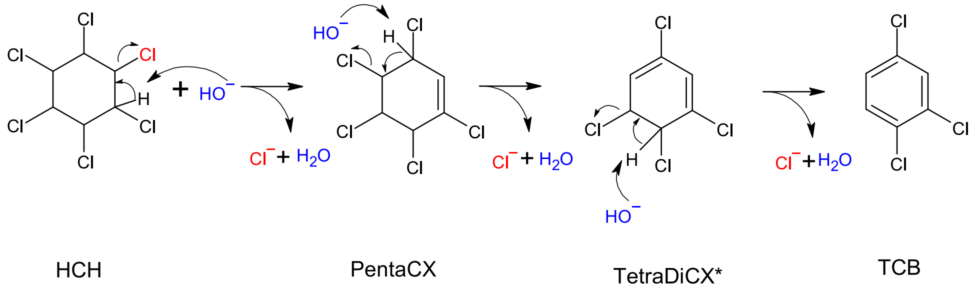

Scheme 1. Reaction mechanism of HCHs dehydrochlorination to PentaCXs and TCBs. The compounds represent the sum of isomers. TetraDiCX isomers were not identified.

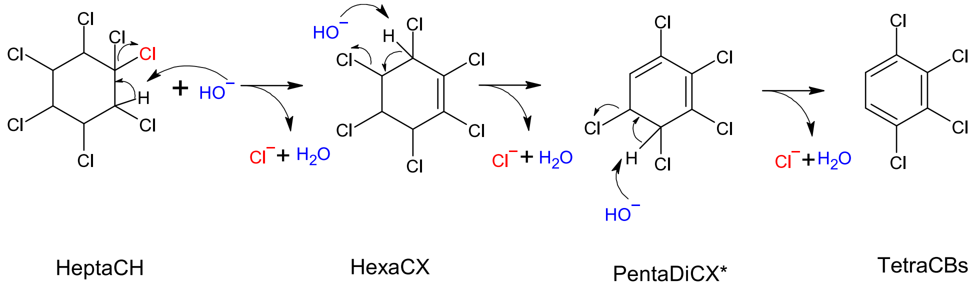

Scheme 2. Reaction mechanism of HeptaCHs dehydrochlorination to HexaCXs and TetraCBS. The compounds represent the sum of isomers. PentaDiCX isomers were not identified.

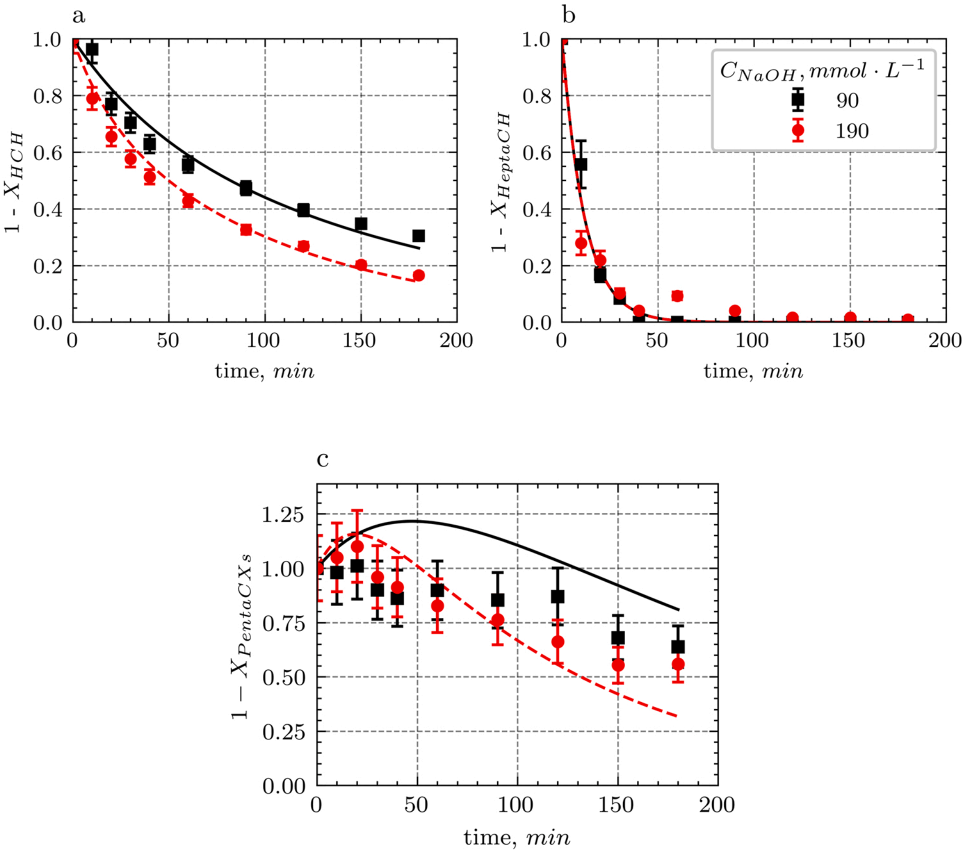

Fig. 5. Remaining fraction of a) HCHs and b) HeptaCH + HexaCX, c) PentaCXs as the sum of isomers varying NaOH concentration. $C_S = 5g\cdot L^{-1}$,$C_{DNAPL} = 500mg\cdot L^{-1}$, $T = 25^{\circ}C$. Symbols depict experimental values and lines the predicted values Eq. (14) to Eq.(23) and parameters in Table 1.

HCHs and PentaCXs are considered separately.

As depicted in Fig. 5, the NaOH concentration increase under the tested experimental conditions results in a slight increase of HCHs hydrolysis rate with a negligible impact on dehydrochlorination of HeptaCH and HexaCX. Moreover, HeptaCH showed a much faster reaction rate.

As Fig. 5c illustrates, the remaining ratio of PentaCX evolution exhibits an initial increase, followed by a decline, reaching a maximum value greater than 1. This behaviour confirmed that PentaCX was generated during the dehydrochlorination of HCH as an intermediate product. The hydrodechlorination rate of PentaCX was barely impacted by alkali concentration. The concentration and time value of the maximum depended on the reaction rate of the dehydrochlorination reaction of HCHs. For these reasons, a positive variation of temperature and NaOH concentration decreased the time and concentration of the maximum point.

Due to the abundance of HCH isomers and the importance of those in the objective of the SEAR treatment in Bailin Landfill, the dehydrochlorination of each HCH isomer ($\alpha,\delta,\gamma, and \varepsilon$) lumped as HCHs in Fig. 5 are shown in Fig. S1. The isomer profiles closely resembled the combined profile of HCHs. Comparing the remaining profiles of isomers, it is discerned that the reaction rates follow the ranking $\delta-HCH > \alpha-HCH > \varepsilon-HCH \approx \gamma - HCH$.

PentaCX and TCBs are the subproducts of HCH, as previously mentioned. Plots of TCB evolutions can be found in Fig. S2a. Furthermore, Fig. S2b shows the concentration change of TetraCBs isomers (a byproduct of HeptaCHs hydrolysis) throughout time. The production ratio is shown in this figure, which is determined by dividing the byproduct's concentration by the total amount of precursor chemicals, as given in Eq. (13). The profiles shown in Fig. S2 are inclined toward one. The latter showed that alkaline conditions did not result in the production of subproducts from TCBs and TetraCBs.

$$Y_j = \frac{\sum C_j}{\sum C_{ko}} \tag{13}$$

where Y_j is the production fraction of the compound j, and C_j and C_{jo} are the concentration in $mmol{\cdot}L^{-1}$ of the isomers at the specific and initial times, respectively. If j = TCBs, then k = HCHs, TCBs, HexaCX and PentaCBs isomers; if j = TetraCBs then k = HeptaCH, HexaCX and TetraCBs isomers.

3.3.3. Effect of the initial concentration of DNAPL in the emulsion

The effect of COCs concentration in the emulsion on the hydrolysis rate of non-aromatic compounds is presented in Fig. 6 for HCHs, HeptaCHs and PentaCXs. As was expected, PentaCX presented a maximum concentration value, and the conversion of non-aromatic COCs was not affected by the initial DNAPL concentration in the emulsion. Therefore, the dehydrochlorination reaction can assume a first-order reaction for COCs concentration. The same conclusion was inferred from the experimental results plotted in Fig. S1, where the conversion profiles of HCH isomers are represented. Fig. S4 shows the concentration profiles of TCBs and TetraCBs isomers.

3.3.4. Effect of surfactant concentration

The effect of surfactant concentration in emulsion on the hydrolysis rate of non-aromatic compounds has been studied in the range 1–10 $g{\cdot}L^{-1}$. The remaining fractional concentration profiles are represented in Fig. 7 for the sum of HCHs, HeptaCHs and PentaCXs. In addition, the shapes of each HCH compound are shown in Fig. S5. It was experimentally found that the DNAPL in the emulsion was not precipitated since the surfactant capacity was kept constant during the reaction time (3 h) in agreement with the reported in previous work (Sáez et al., 2022a).

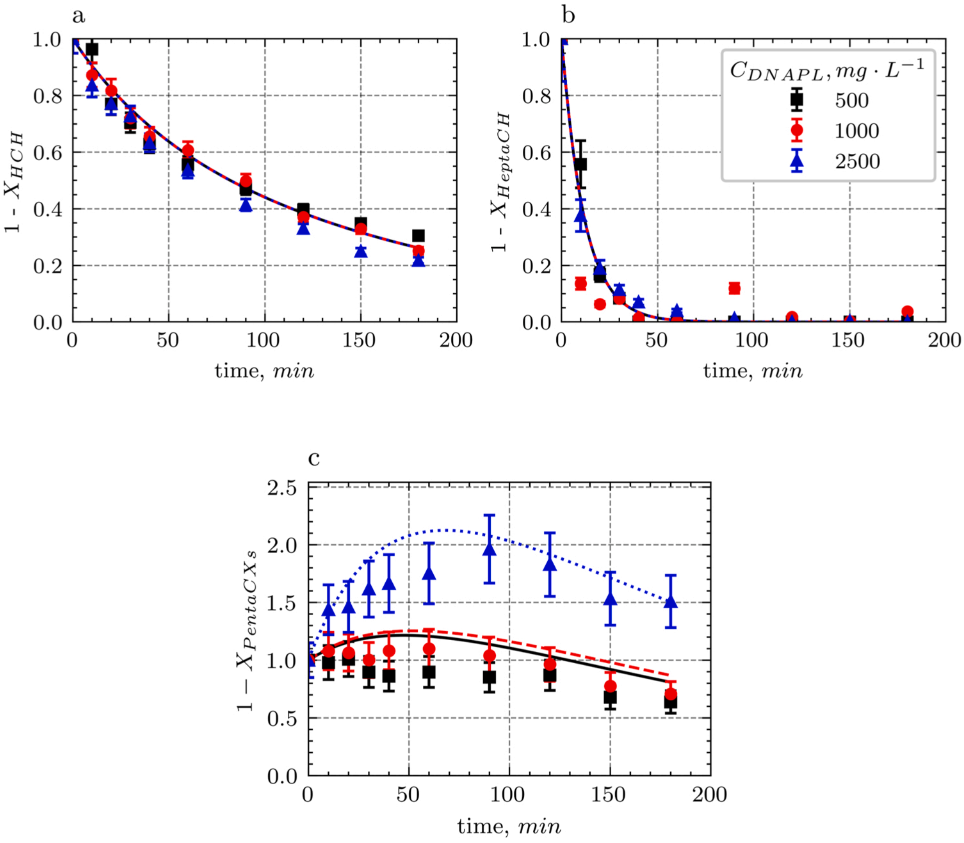

Fig. 6. Remaining fraction of of a) HCHs and b) HeptaCH + HexaCX, c) PentaCXs as the sum of isomers varying the DNAPL initial concentration. $C_S = 5g{\cdot}L^{-1}, C_{NaOH} = 90mmol{\cdot}L^{-1}, T = 25°C$. Symbols depict experimental values and lines the predicted values Eq. (14) to Eq.(23) and parameters in Table 1.

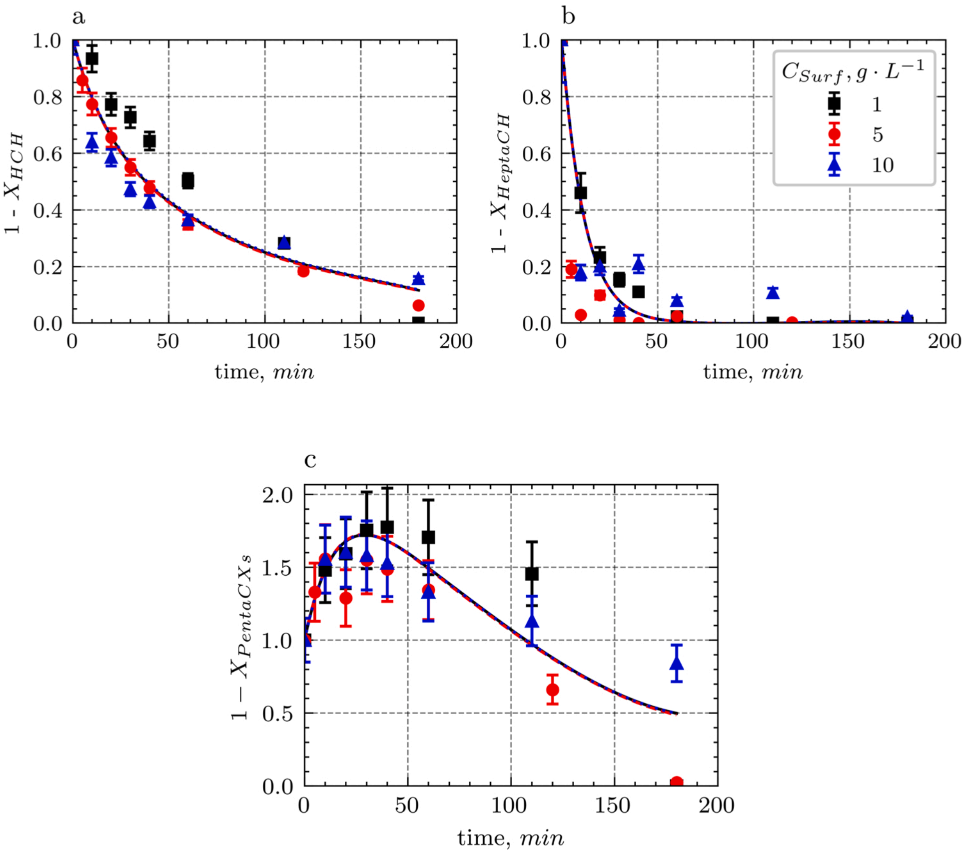

Fig. 7. Remaining fraction of of a) HCHs and b) HeptaCH + HexaCX, c) PentaCXs as the sum of isomers varying the surfactant concentration. $C_{DNAPL} = 1000 mg{\cdot}L^{-1}$, $C_{NaOH} = 90 mmol{\cdot}L^{-1}, T = 25°C$. Symbols depict experimental values and lines the predicted values Eq. (14) to Eq.(23) and parameters in Table 1.

The experimental results proved that, in the range studied, the surfactant concentration did not affect the dehydrochlorination reaction rate.

The concentration of the final products (TCBs, TetraCBs) of the dehydrochlorination reaction are shown in Fig. S6. The surfactant concentration showed again a negligible influence in the byproducts profile.

3.3.5. *Effect of temperature*

The dehydrochlorination of HCH isomers was investigated at different temperatures; the results are presented in Fig. 8a. As expected, the higher the temperature, the higher the HCH reaction rate. The influence of temperature on the dehydrochlorination reaction was also examined for each HCH isomers. As experimentally demonstrated in Fig. S7, temperature positively impacted the reaction rate of these isomers.

The dehydrochlorination rate of heptachlorohexane (HeptaCH) by alkali was excessively rapid, making it challenging to discern any significant influence of temperature at temperatures above 313 K, as depicted in Fig. 8b.

The temperature-dependent concentration profile of PentaCX is illustrated in Fig. 8c. As the temperature increases, the time needed to reach the maximum decreases, accompanied by an elevated rate of disappearance of these compounds. In addition, the maximum concentration value increased with the temperature, as was experimentally probed in data represented in Fig. 8c. The latter can be explained if the active energy of the dehydrochlorination reaction of PentaCX to produce TCB is lower than the activation energy of the dehydrochlorination reaction of HCH to produce PentaCX following a serial reaction mechanism (as is discussed later). This observation confirms that temperature positively impacts the formation of these compounds from HCHs and their subsequent transformation into TCBs. Fig. S8 shows the concentration profiles of PentaCX, TCBs, and TetraCBs.

3.3.6. *Kinetic model of dehydrochlorination reaction*

The experimental findings from Set-B (Table S4), were employed to formulate a kinetic model capable of elucidating the influences of temperature, NaOH, surfactant and COCs concentration on the dehydrochlorination rate of non-aromatic COCs. Subsequently, kinetic parameters were obtained through data fitting. Grounded in the experimental results, the following assumptions were considered:

- The dehydrochlorination rate of HCH and HeptaCH isomers is promoted by alkali. However, the effect NaOH concentration was negligible under the experimental conditions tested.
- The dehydrochlorination rate follows a first-order reaction on HCH and lumped HeptaCH + HexaCX isomers concentration since the conversion of those compounds did not depend on their initial concentration in the emulsion.
- The dehydrochlorination rate does not depend on the HCH and HeptaCH + HexaCX isomer surfactant concentration.
- The positive effect of temperature was observed for the dehydrochlorination of HCH but could not be quantified for HeptaCH + HexaCX due to their fast dehydrochlorination rate.

3.3.6.1. *Kinetic model for HCH isomers dehydrochlorination.* The kinetic model of the dehydrochlorination reaction of HCH isomers was proposed for $\alpha - HCH, \gamma - HCH, \delta - HCH, \varepsilon - HCH$. As proposed in Scheme 1, those compounds reacted, producing PentaCX isomers as their sum. Then, PentaCX reacted to produce TCB isomers according to the reaction summarised in Eqs. (14) and (15).

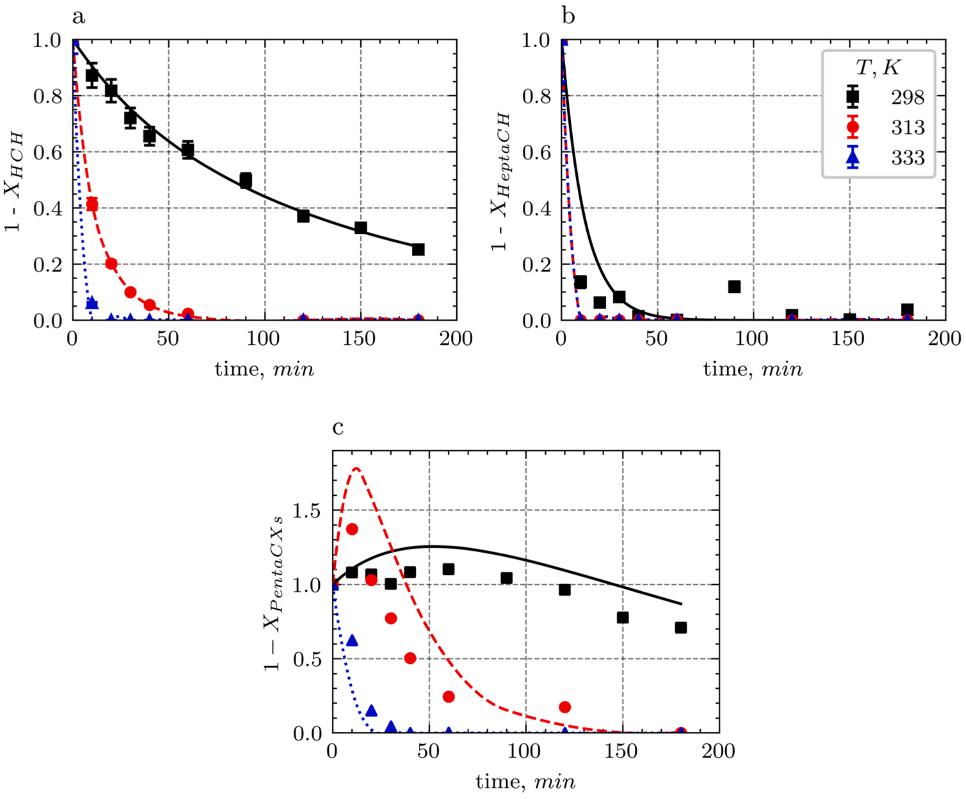

Fig. 8. Remaining fraction of of a) HCHs and b) HeptaCH + HexaCX, c) PentaCXs as the sum of isomers varying the temperature. $C_{DNAPL} = 1000 mg \cdot L^{-1}, C_{NaOH} = 90 mmol \cdot L^{-1}, C_{surf} = 5 g \cdot L^{-1}$. Symbols depict experimental values and lines the predicted values Eq. (14) to Eq.(23) and parameters in Table 1.

$$r_1 : HCH + NaOH \rightarrow PentaCX + NaCl + H_2O \tag{14}$$

$$r_2 : PentaCX + 2NaOH \rightarrow TCBs + 2NaCl + 2H_2O \tag{15}$$

The mass balances in the reaction of HCHs to TCBs are summarised in Eqs. (16)–(18).

$$\frac{dC_{HCH_k}}{dt} = -r_{1k} \mathrm{k} \in \{\alpha - HCH, \gamma - HCH, \delta - HCH, \varepsilon - HCH\} \tag{16}$$

$$\frac{dC_{PentaCX_k}}{dt} = \sum r_{1k} - \mathrm{r}_2 \tag{17}$$

$$\frac{dC_{TCBs_k}}{dt} = r_2 \tag{18}$$

being C_{HCH_k} the concentration in ($mmol \cdot L^{-1}$) of each isomer of HCH, $C_{PentaCX_k}$ and C_{TCBs_k} the concentrations of the sum of isomers of PentaCX and TCBs, respectively, at a time t. Here, r_{1k} (in $mmol \cdot L^{-1} \cdot \mathrm{min}^{-1}$) is the velocity of the reaction in Eq. (14). It depends on the HCH isomers, and the model is in Eq. (19). A unique rate is defined for the reaction in Eq. (15) to express the reaction of PentaCX as a lumped compound of isomers. The kinetic model proposed for this reaction is summarised in Eq. (20).

$$r_{1k} = k_{1k} \cdot C_{NaOH}^{n} \cdot C_{HCH} \tag{19}$$

$$r_2 = k_2 \cdot C_{NaOH}^{n} \cdot C_{PentaCX} \tag{20}$$

Here C_{NaOH} is the NaOH concentration ($g \cdot L^{-1}$); k are the reaction rate constants ($L^n \cdot mmol_{NaOH}^{-n} \cdot \mathrm{min}^{-1}$). The constants consider the temperature effect following the Arrhenius law (Levenspiel, 1999), expressed in Eq. (21).

$$k_k = k_{k0} \cdot \exp\left(-\frac{Ea_k}{T(K)}\right) \tag{21}$$

3.3.6.2. Kinetic model for HeptaCH + HexaCX (lumped compound) dehydrochlorination. The dehydrochlorination of HeptaCH and HexaCX summarised in Scheme 2, was assumed as a one-step reaction to produce the TetraCBs isomers, as is shown in Eq. (22). The mass balance and the kinetic model proposed are summarised in Eq. (23)

$$r_3 : (HeptaCH + HexaCX) + 3NaOH \rightarrow TetraCBs + 3NaCl + 3H_2O \tag{22}$$

$$\frac{dC_{HeptaCH+HexaCX}}{dt} = -r_3 = -k_3 \cdot C_{HeptaCH+HexaCX} \tag{23}$$

Data from experiments in Set-B were fitted to the model in Eqs. (14)–(23). The problem to be solved is composed of a mixed set of differential and algebraic equations. It was implemented in ModelBuilder 7.1.0 provided in the gPROMS suit and the algorithm DASOLV was used to simulate the reaction system. DASOLV is based on a variable time step, variable order and Backward Differentiation Formulae (BDF) (Siemens, 2022). The estimated parameters calculated for the SCL kinetic model minimising the sum of quadratic residuals (SQR) in Eq. (24) are shown in Table 1, with the confidence interval (CI) (95 %) of the parameters.

$$SQR = \sum \left(C_{j \quad \exp} - C_{j \quad pred}\right)^2 \quad \left(mg \cdot L^{-1}\right)^2 \tag{24}$$

The predicted values of the conversion of HCH and HeptaCH + Hexa isomers using the model in Eqs. (14)–(23) and the parameters gathered in Table 1 are represented from Fig. 5 to Fig. 8. The conversion values predicted for each HCH isomer and the corresponding concentrations of TCBs and TetraCBs are represented as lines from Fig. S1 to Fig. S7 and at 298 K in Fig. S8. The excellent agreement between the observed and predicted conversions and concentration values inferred that the proposed kinetic model could adequately predict the dehydrochlorination of non-aromatic compounds in the DNAPL.

It is worth noting that the model had challenges accurately predicting the experimental results depicted in Fig. S8 at 313 K and 333 K. As observed, the experimental values were lower than expected at both temperatures, likely due to the losses of TCBs and TetraCBs by

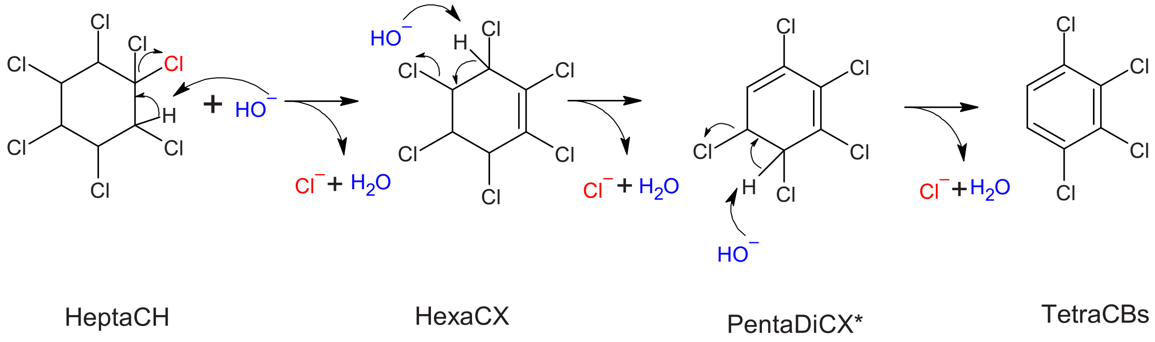

Table 1
Kinetic parameters were obtained by fitting the model expressed in Eqs. (14)–(23) to the experimental data obtained in Set-B.

	$\alpha - HCH,$	$\gamma - HCH,$	$\delta - HCH$	$\varepsilon - HCH$
Ea_1, K	13956 ± 143	14710 ± 50	14891 ± 946	17841 ± 918
$\exp(k_{o1}), \mathrm{min}^{-1}$	39 $\pm 4{\cdot}10^{-3}$	41 $1{\cdot}10^{-4}$	41 $6{\cdot}10^{-4}$	51 0.6
m	0.61 ± 0.002	0.57 $\pm 3{\cdot}10^{-5}$	1.06 $1{\cdot}10^{-3}$	0.61 0.17
SQR, $(mmol{\cdot}L^{-1})^2$	9.11	4.73	15.28	1.67
Ea_2, K	14065.9 ± 36			
$k_{o2}, \mathrm{min}^{-1}$	37.7609 ± 0.12			
m	0.98 $\pm 2.1 \times 10^{-5}$			
SQR$(mmol{\cdot}L^{-1})^2$	10.5			
k_3, min^{-1}	0.083 ± 0.008			
SQR$(mg{\cdot}L^{-1})^2$	87.2			

evaporation.

3.4. Validation

The experimental concentrations of DNAPL, surfactant and COCs in Set-A experiments are shown as symbols in Fig. 2 to Fig. 4, respectively. The lines in those charts represent the predicted values by the model presented in the previous sections. A good agreement was found between experimental and predicted values for experiments PP-1 and PP-2, carried out at the pilot plant scale. The latter validated the model proposed, which can be used to model the unit to treat emulsion composed of COCs by coupling vaporisation and dehydrochlorination.

In the case of the ESC represented in Fig. 2b, the experimental results are better explained, assuming the residual ESC was negligible for PP-1 and PP-2, using $x_r = 0$ in Eq. (12).

4. Conclusions

The treatment of real emulsions obtained after the application of SEAR within the framework of the LIFE SURFING project, through the combination of hydrolysis of non-aromatic compounds to generate aromatic compounds with lower boiling points and subsequent vaporisation of these compounds, has proven to be highly effective. Removal rates of chlorinated compounds exceeding 95 % were obtained within 25 h of treatment.

Designing the emulsion treatment process required the development of a kinetic model for the dehydrochlorination of HCH, PentaCX, HeptaCH and HexaCX isomers to produce TCBs and TetraCBs isomers. The influence of NaOH concentration, surfactant, initial DNAPL and temperature was studied, concluding that the most influential variables are NaOH concentration and temperature. Model parameters were fine-tuned using experimental data, accounting for the temperature and NaOH concentration effects.

This kinetic model developed in this work and the model for vaporising aromatic compounds found elsewhere were successfully validated in treating actual emulsions containing COCs. These findings provide a valuable tool for simulating and optimising the treatment process of contaminated emulsions, contributing to environmental science and technology advancement.

Declaration of Competing Interest

The authors declare that they have no known competing financial interests or personal relationships that could have appeared to influence the work reported in this paper.

Acknowledgements

This work was supported by the EU Life Program (LIFE17 ENV/ES/000260) and Spanish Ministry of Economy, Industry and Competitiveness, through the Projects PID2022-137828OB-I00 and PDC2022-133095-I00.

Appendix A. Supporting information

Supplementary data associated with this article can be found in the online version at doi:10.1016/j.psep.2024.01.083.

References

Aidoo, O.F., Osei-Owusu, J., Chia, S.Y., Dofuor, A.K., Antwi-Agyakwa, A.K., Okyere, H., Gyan, M., Edusei, G., Ninsin, K.D., Duker, R.Q., Siddiqui, S.A., Borgemeister, C., 2023. Remediation of pesticide residues using ozone: a comprehensive overview. Sci. Total Environ. 894, 164933.

Araújo, M.F., Castanheira, E.M.S., Sousa, S.F., 2023. The buzz on insecticides: a review of uses, molecular structures, targets, adverse effects, and alternatives. Molecules 28, 3641.

Bescós, A., Herrerías, C.I., Hormigón, Z., Mayoral, J.A., Salvatella, L., 2021. Theoretical insight on the treatment of β-hexachlorocyclohexane waste through alkaline dehydrochlorination. Sci. Rep. 11, 8777.

Bouzid, I., Maire, J., Laurent, F., Broquaire, M., Fatin-Rouge, N., 2021. Controlled treatment of a high velocity anisotropic aquifer model contaminated by hexachlorocyclohexanes. Environ. Pollut. 268.

Dominguez, C.M., Romero, A., Santos, A., 2019. Selective removal of chlorinated organic compounds from lindane wastes by combination of nonionic surfactant soil flushing and Fenton oxidation. Chem. Eng. J. 376.

Duttagupta, S., Mukherjee, A., Bhattacharya, A., Bhattacharya, J., 2020. Wide exposure of persistent organic pollutants (PoPs) in natural waters and sediments of the densely populated Western Bengal basin, India. Sci. Total Environ. 717, 137187.

Garcia-Cervilla, R., Santos, A., Romero, A., Lorenzo, D., 2021. Partition of a mixture of chlorinated organic compounds in real contaminated soils between soil and aqueous phase using surfactants: influence of pH and surfactant type. J. Environ. Chem. Eng. 9, 105908.

García-Cervilla, R., Romero, A., Santos, A., Lorenzo, D., 2020. Surfactant-enhanced solubilization of chlorinated organic compounds contained in dnapl from lindane waste: Effect of surfactant type and ph. Int. J. Environ. Res. Public Health 17, 1–14.

García-Cervilla, R., Santos, A., Romero, A., Lorenzo, D., 2021. Compatibility of nonionic and anionic surfactants with persulfate activated by alkali in the abatement of chlorinated organic compounds in aqueous phase. Sci. Total Environ. 751, 141782.

Hanafiah, S.A., Mohamed, M.A., Caradec, S., Fatin-Rouge, N., 2018. Treatment of heavy petroleum hydrocarbons polluted soil leachates by ultrafiltration and oxidation for surfactant recovery. J. Environ. Chem. Eng. 6, 2568–2576.

Huan, J.C., Shang, C., 2006. Air Stripping. In: Wang, L.K., Hung, Y.T., Shammas, N.K. (Eds.), Advanced Physicochemical Treatment Processes. Handbook of Environmental Engineering, Vol. 4. Humana Press.

Huo, L., Liu, G., Yang, X., Ahmad, Z., Zhong, H., 2020. Surfactant-enhanced aquifer remediation: Mechanisms, influences, limitations and the countermeasures. Chemosphere 252, 126620.

Ingold, C., 1953. Structure and Mechanism in Organic Chemistry. Cornell University Press.

Levenspiel, O., 1999. Chemical Reaction Engineering. Wiley.

Li, S., Elliott, D.W., Spear, S.T., Ma, L., Zhang, W.-X., 2011. Hexachlorocyclohexanes in the environment: mechanisms of dechlorination. Crit. Rev. Environ. Sci. Technol. 41, 1747–1792.

Lorenzo, D., García-Cervilla, R., Romero, A., Santos, A., 2020. Partitioning of chlorinated organic compounds from dense non-aqueous phase liquids and contaminated soils from lindane production wastes to the aqueous phase. Chemosphere 239.

Negrete-Bolagay, D., Zamora-Ledezma, C., Chuya-Sumba, C., De Sousa, F.B., Whitehead, D., Alexis, F., Guerrero, V.H., 2021. Persistent organic pollutants: the trade-off between potential risks and sustainable remediation methods. J. Environ. Manag. 300, 113737.

Rosas, J.M., Santos, A., Romero, A., 2013. Soil-washing effluent treatment by selective adsorption of toxic organic contaminants on activated carbon. Water Air Soil Pollut. 224, 10.

Sáez, P., García-Cervilla, R., Santos, A., Romero, A., Lorenzo, D., 2022a. Treatment of a complex emulsion of a surfactant with chlorinated organic compounds from lindane wastes under alkaline conditions by air stripping. Ind. Eng. Chem. Res.

Sáez, P., Santos, A., García-Cervilla, R., Romero, A., Lorenzo, D., 2022b. Non-ionic surfactant recovery in surfactant enhancement aquifer remediation effluent with chlorobenzenes by semivolatile chlorinated organic compounds volatilization. Int. J. Environ. Res. Public Health 19.

Santos, A., Fernandez, J., Guadano, J., Lorenzo, D., Romero, A., 2018. Chlorinated organic compounds in liquid wastes (DNAPL) from lindane production dumped in landfills in Sabinanigo (Spain). Environ. Pollut. 242, 1616–1624.

Santos, A., Domínguez, C.M., Lorenzo, D., García-Cervilla, R., Lominchar, M.A., Fernández, J., Gómez, J., Guadaño, J., 2019. Soil flushing pilot test in a landfill polluted with liquid organic wastes from lindane production. Heliyon 5, e02875.

Siemens, 2022. Process Systems Enterprise, gPROMS.

Trinh, T.A., Han, Q., Ma, Y., Chew, J.W., 2019. Microfiltration of oil emulsions stabilized by different surfactants. J. Membr. Sci. 579, 199–209.

Vane, L.M., Giroux, E.L., 2000. Henry's law constants and micellar partitioning of volatile organic compounds in surfactant solutions. J. Chem. Eng. Data 45, 38–47.

Verma, D.K., Dewangan, Y., Verma, C., 2023. Chapter 1 - Organic reaction mechanism. In: Verma, D.K., Dewangan, Y., Verma, C. (Eds.), Handbook of Organic Name Reactions. Elsevier, pp. 1–153.

Zhang, Z., Zhou, Z., Liu, X., Zhang, H., Xu, H., Lin, C., He, M., Ouyang, W., 2023. Mechanochemical remediation of lindane-contaminated soils assisted by CaO: performance, mechanism and overall assessment. J. Hazard. Mater. 458, 131985.